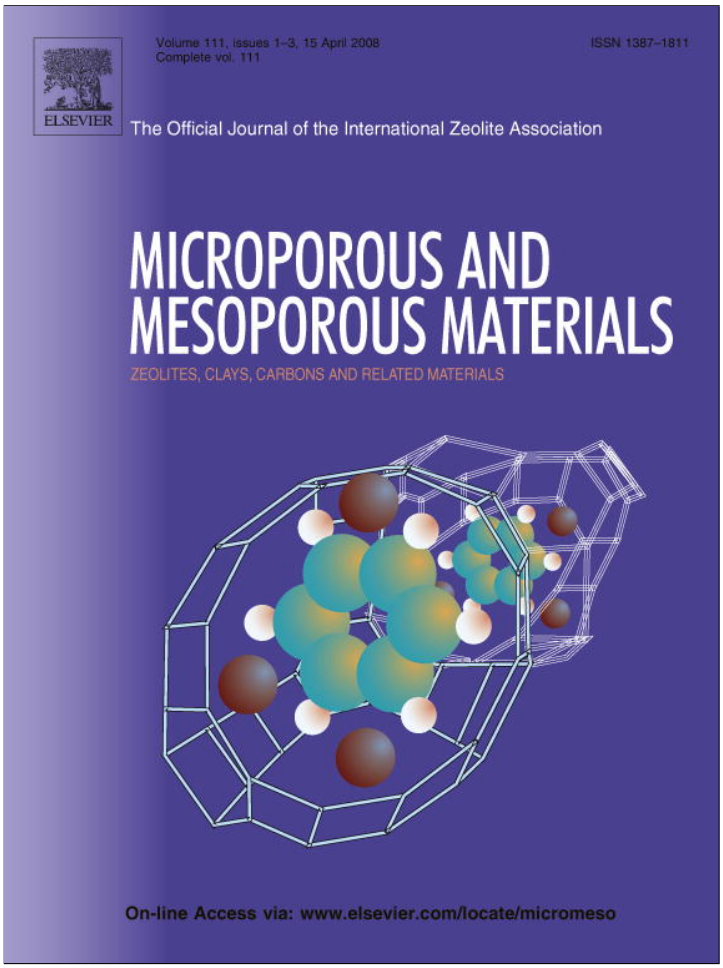

Available online at www.sciencedirect.com
ScienceDirect
Microporous and Mesoporous Materials 111 (2008) 620–626
MICROPOROUS AND MESOPOROUS MATERIALS
www.elsevier.com/locate/micromeso

Short Communication

Effect of the flowing gases of steam and CO_2 on the texture and catalytic activity for methane combustion of MgO powders

Fei Teng [a], Wei Qu [b], Guodong Wen [b], Zheming Wang [b], Zhijian Tian [b], Xiaomei Yang [b], Ping Xu [b], Yongfa Zhu [a,*], Guoxing Xiong [b]

[a] *Department of Chemistry, Tsinghua University, Beijing 100084, China*
[b] *State Key Laboratory of Catalysis, Dalian Institute of Chemical Physics, Dalian 116023, China*

Received 20 May 2007; received in revised form 10 July 2007; accepted 12 July 2007
Available online 19 July 2007

Abstract

In this work, the MgO powders was prepared by the precipitation method with carbonate following calcination at 1200 °C, and then the obtained MgO powders was treated under the flowing gaseous mixture of steam and CO_2. The variations of textural properties and activity for methane combustion of the MgO sample were investigated. The sample was characterized by N_2 adsorption isotherm, TEM, XRD, and TG-DTA. The results showed that the treatment temperature and the CO concentration have a significant influence on the textural properties of the MgO sample. After run at 700 °C for 24 h under the flowing gaseous mixture of steam/CO_2/N_2 (CO_2/N_2 = 15/85 volume ratio), the maximum pore sizes varied and the pore volumes increased obviously; and remarkably, the surface area of the MgO sample increased from 37.9 to 80.1 $m^2\ g^{-1}$. It was proposed that during the process, the disaggregation and rearrangement of the particles have occurred, leading to the obvious variations of the textural properties of the sample. As a result, the treated MgO sample showed a higher activity for methane combustion than the original one.

Keywords: MgO; CO_2/H_2O; Pore size distribution; Surface area; Methane combustion

1. Introduction

Catalytic combustion of natural gas has many advantages over the conventional flame combustion in suppressing emissions (NO_x, CO) and improving energy efficiency [1]. However, the catalysts/supports with high thermal stability are needed for the high-temperature combustion of methane. MgO is an important material, which has been widely employed as catalyst support, reinforcing reagent, as well as a component in superconductors [2–4]. MgO has been considered as one of the most stable materials for methane combustion at high temperatures due to its high melting point. However, the significant amounts of CO_2 and steam are produced in the process of methane combustion, which would have an influence on the catalyst properties considering the intrinsic acid/base properties of CO_2 and MgO [5]. The adsorption and catalytic behaviors are usually related to their textural and surface properties of the materials. The textural properties of the materials, e.g., porosity, surface area and particle size, are the very important parameters of the catalysts/supports, and these properties are strongly dependent on the preparation [6–10]. However, little work has been performed to study the variations of the textural properties of the MgO sample in the presence of CO_2 and H_2O.

In this work, the variations of textural properties of the MgO sample under the flowing gaseous mixture of steam and CO_2 were investigated. This treatment was used to simulate the combustion conditions of methane, in which the significant amounts of steam and CO_2 were present. The

* Corresponding author. Tel./fax: +86 10 62787601.
E-mail addresses: teng-fei@mail.tsinghua.edu.cn (F. Teng), zhuyf@mail.tsinghua.edu.cn (Y. Zhu).

1387-1811/$ - see front matter © 2007 Elsevier Inc. All rights reserved.
doi:10.1016/j.micromeso.2007.07.013

morphology, crystal structure and textural properties of the samples were characterized by TEM, XRD, N_2 adsorption isotherm and TG-DTA. An interaction mechanism in this process was proposed, and the effect of the treatment method on the activity of methane combustion over the MgO sample was also investigated.

2. Experimental

2.1. Preparation and treatment of the MgO sample

In this experiment, all the chemicals, including $Mg(NO_3)_2 \cdot 6H_2O$ (A.R.), $(NH_4)_2CO_3$ (A.R.), and Span80 (A.R. sorbitan monooleate, $C_{24}H_{44}O_6$, MW = 428), were purchased from Beijing Chemicals Company of China and used as received.

At room temperature, the MgO powder was prepared by precipitating of magnesium nitrate with ammonia carbonate in the presence of Span80. Span80 was used to refrain the particle agglomeration. If the surfactant (e.g., Span80) was not used, the MgO sample calcined at 1200 °C for 5 h generally has lower surface areas (10–15 $m^2 g^{-1}$), which showed a low activity for methane combustion. Typically, an amount of Span80 (0.025 mol, 11.2 g) was added to 100 mL 0.5 mol L^{-1} $Mg(NO_3)_2$ aqueous solution, and the mixture was stirred for 10 min. Hundred milliliters of 1.0 mol L^{-1} $(NH_4)_2CO_3$ aqueous solution was added dropwise to the above solution under stirring. After stirred for another 2 h, the mixture was aged for 24 h at room temperature. Finally, the solid was separated by centrifuging, and washed with water for three times. The sample was dried at 110 °C for 24 h in an oven. The precursor was calcined at 500 °C for 5 h to remove the surfactant, and further calcined at 1200 °C for 5 h.

The MgO sample calcined at 1200 °C for 5 h was treated at 500 or 700 °C for the different intervals under the gaseous mixture of steam and CO_2. Typically, 1.0 g of MgO powder was put in a quartz reactor and run at a space velocity of 1200 h^{-1}. The gaseous mixture was obtained by passing CO_2/N_2 (5/95 and 15/85 volume ratio) through boiling water to carry water vapor.

2.2. Characterization

The samples were characterized by X-ray diffraction (XRD) on a Rigaku D/MAX-RB X-ray powder diffractometer, using graphite monochromatized Cu Kα radiation ($\lambda = 0.154$ nm), operating at 40 kV and 50 mA. The patterns were scanned from 10° to 70° (2θ) at a scanning rate of 5° min^{-1}. A nitrogen adsorption isotherm was performed at 77 K on a Micromeritics ASAP2010 gas adsorption analyzer. Each sample was degassed at 200 °C for 5 h before the measurement. Surface area and pore size distribution were calculated by BET (Brunauer–Emmett–Teller) and BJH (Barrett–Joyner–Halenda) methods, respectively. The morphology of the catalyst was characterized with a JEOL model 200CX transmission electron microscope with the accelerating voltage of 200 kV. The powders were dispersed in ethanol ultrasonically, and then the samples were deposited on a thin amorphous carbon film supported by copper grids. TGA-DTA was carried out with Pyris 1 TGA thermogravimeter and DTA-7 (US Perkin–Elmer Co.), and the temperature rises from room temperature to 900 °C at a rate of 10 °C min^{-1}.

2.3. Catalytic combustion of CH_4

The combustion of CH_4 was conducted in a conventional flow system at atmospheric pressure. The catalyst (0.1 g) was diluted with quartz powder (0.1 g), and loaded in a quartz reactor (i.d. 5 mm) with quartz beads packed at both ends of the catalyst bed. The thermal couple was placed in the catalyst bed to monitor the reaction temperature since CH_4 combustion is an exothermic reaction. Before each run, the catalyst was flushed with air (100 mL min^{-1}) at 500 °C for 1 h in order to remove adsorbed species from the surface, and then cooled to 200 °C. A gas mixture of 1 vol% CH_4 and 20 vol% O_2 (balanced with Ar) was fed into the catalyst bed at a GHSV (gas hourly space velocity) of 100,000 h^{-1}. The inlet and outlet gas compositions were analyzed by an on-line gas chromatograph with a packed column of carbon molecular sieve (1.5 m × 4 mm) and a thermal conductivity detector (TCD).

3. Results and discussion

3.1. The variations of textural properties and particle sizes of the MgO samples

Table 1 shows the textural properties of the original and treated MgO samples. The BET surface area of the original MgO sample (M0) is 37.9 $m^2 g^{-1}$. After treatment at 500 °C for 24 h under the flowing gaseous mixture of steam/CO_2/N_2 ($CO_2/N_2 = 5/95$ volume ratio), the BET surface area (38.5 $m^2 g^{-1}$) of the MgO sample (M1) did not vary, considering the analysis error range of the measure method. It is evident that the mild treatment, at a low concentration of CO_2 and a low temperature, has no

Table 1
Textural properties of the MgO samples before and after treatment with a mixture of steam and CO_2

Sample	Treatment (°C/h)	SA[a] ($m^2 g^{-1}$)	V_{pore}[a] ($cm^3 g^{-1}$)	d_{pore}[a] (nm)
M0	–	37.9	0.10	2.8
M1	500/24[b]	38.5	–	–
M2	700/12[c]	40.1	0.13	2.8, 18
M3	700/24[c]	80.1	0.19	3.9

[a] SA, Surface area calculated by the BET method; V_{pore}, pore volume; d_{pore}, maximum value of pore size distribution calculated by BJH method; running under the flowing gaseous mixture of steam/CO_2/N_2.
[b] $CO_2/N_2 = 5/95$ (volume ratio).
[c] $CO_2/N_2 = 15/85$ (volume ratio).

significant influence on the textural properties of the MgO sample.

To observe the texture variations, the MgO sample were treated under the severe conditions, i.e., by increasing CO_2 concentration and run temperature. Fig. 1. shows the sorption isotherms and pore size distributions of the sample before and after treated at 700 °C for 12 h under the flowing mixture gases of steam/CO_2/N_2 (CO_2/N_2 = 15/85 volume ratio). According to the IUPAC classification [11], the original (M0) and the treated (M2) samples showed the similar sorption isotherms. They are both "type II" isotherms with the peculiar hysteresis loops and are apparently not mesoporous ordered (type IV). Their pores seem to result from the interparticle voids in the wide size range, in line with the extremely broad pore size distribution. It is interesting that after treatment, the pore volume of M2 sample increased significantly from 0.10 to 0.13 $cm^3\ g^{-1}$ (Fig. 1a), and the double peaks in pore size distribution appear at 2.8 and 18 nm, respectively. Note that for M2 sample, the new pores of 18 nm generated while the pores of 2.8 nm were reduced obviously. This is much different from the single peak (2.8 nm) distribution of the original sample (Fig. 1b). However, the BET surface area of the MgO sample increased slightly (37.9 vs. 40.1 $m^2\ g^{-1}$). It seems that the severe treatment has a significant influence on the textural properties of the sample. The occurrence of the maxima at 18 nm in the pore size distribution in M2 samples is understandable. If we observe the locally enlarged isotherms, there is still a little difference in these isotherms. We could assume that after being attached by steam and CO_2, the agglomerated secondary particles may have disaggregated and further rearranged to form the smaller particles and some smaller particles may have grown into larger ones. As a result, the maximum pores of 18 nm may be generated from the voids among these secondary particles. The maximum pores at 2.8 nm may result from the interstices among the primary particles (i.e., within the secondary particles), and the maximum

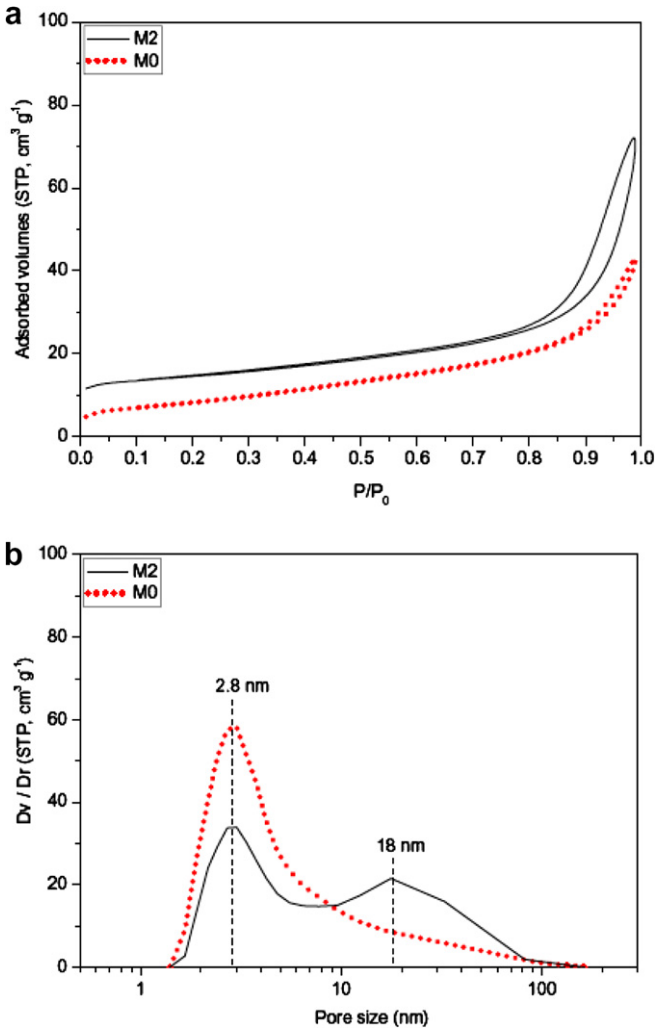

Fig. 1. N_2 adsorption–desorption isotherms (a) and pore size distributions (b) of MgO samples: M0, the original MgO sample; M2, after treatment at 700 °C for 12 h under the flowing gaseous mixture of steam/CO_2/N_2 (CO_2/N_2 = 15/85 volume ratio).

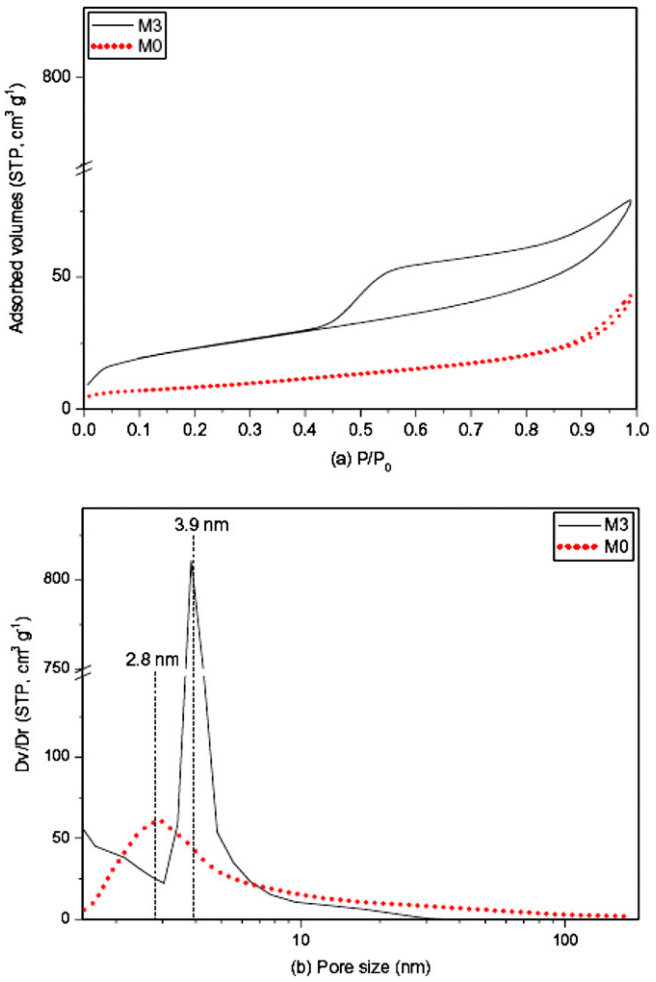

Fig. 2. N_2 adsorption–desorption isotherms (a) and pore size distributions (b) of MgO samples: M0, the original MgO sample; M3, after treatment at 700 °C for 24 h under the flowing gaseous mixture of steam/CO_2/N_2 (CO_2/N_2 = 15/85 volume ratio).

pores at 18 nm may result from the interstices among the small secondary particles.

Further, the original MgO sample was processed with the mixture gases of steam/CO_2/N_2 (CO_2/N_2 = 15/85, volume ratio) at 700 °C for 24 h. As shown in Fig. 2a, the N_2 adsorption isotherms on the MgO sample (M3) exhibit a classical type IV adsorption isotherm with a H_2-hysteresis loop, according to the IUPAC classification [11], which indicates the crossed pores with narrow necks and wide bodies (often referred to as 'inkbottle' model mesopores) were formed. The isotherms of M3 are clearly different from those of the original sample (M0). Interestingly, although the pore size distribution of M3 is still wide, their pore sizes are clearly different from those of the original sample (M0). Compared with the original sample (M0), the new mesopores with 3.9 nm maximum are generated, accompanied by the decrease of the large pores (>30 nm) but the slight increase of the partial micropores (<1.5 nm). The increase of micropores may be the migration of Mg with steam, although we could not give the direct proof limited by our experiment conditions. We could assume that in the presence of steam and CO_2, the migration of Mg ions with steam would occur, and the migration of Mg from the surface of MgO crystal would lead to the generation of new micropores in the remained particles. This could be supported by the coarseness of the grain surface on base of the TEM micrographs in Fig. 3 (in the next part). Therefore, the micropores increased. This may also favor for the increase of the BET area, which has been observed in Table 1 and Fig. 2. On the other hand, the migrated Mg would form new grains and/or aggregate into the secondary particles. Furthermore, the disaggregated grains by the mixture gases further rearranged to form the new interstice. As a result, the maximum of pore size distribution shifts to 3.9 nm and the pore size distribution also becomes narrower slightly, which is much different from that (wide, centered at 2.8 nm) of the M0 sample (Fig. 2b). Most importantly, after treatment for 24 h, the surface area of the MgO sample (M3) increased greatly to 80.1 $m^2\ g^{-1}$, which is much higher than that (37.9 $m^2\ g^{-1}$) of the original sample (M0) (shown in Table 1). The increase of the surface area of the MgO sample may be ascribed as to the generation of the new mesopores, as well as the increase of micropores.

The particle morphologies of the original and the treated MgO samples were observed with TEM (Fig. 3). Before treatment, the original MgO particles (M0) agglomerated severely, and the particle size was large with a wide size distribution (from 100 nm to several microns) (Fig. 3a). After treatment at 700 °C for 12 h under the flowing mixture gases of steam/CO_2/N_2 (CO_2/N_2 = 15/85, volume ratio), the agglomeration of the particles was alleviated to some extent. As shown in Fig. 3b (the arrow indicated), some particles disaggregated and their surface became coarse clearly, although the morphology variations of most of the particles can not be discerned clearly. This may be due to the short treatment duration. As the time of treatment was elongated to 24 h, the agglomeration of the particles was relieved clearly, and their particle sizes became much smaller (50–100 nm) than those of the original sample (Fig. 3c). It is evident that such a treatment has also an obvious influence on the particle size.

3.2. The proposed interaction mechanism

From the results above, it has been found clearly that after treatment, the BET area of M3 sample increased about one time and the pore volume increased, compared with the original sample (M0). Although the pore size distribution is still wide, the maximum of pore size distribution has shifted to larger by the treatment. This firmly demonstrated that the treatment has a significant influence on the texture properties of the sample. To understand this process, TG-DTA was performed to investigate the thermal properties of the carbonate precursor after being dried at 100 °C. Observed from Fig. 4, three peaks of weight loss can be found in TG curve. Firstly, a slight weight loss (5 wt%) in the rang of from 50 to 250 °C was caused by the dehydration and dehydroxylation, which is accompanied by a slight

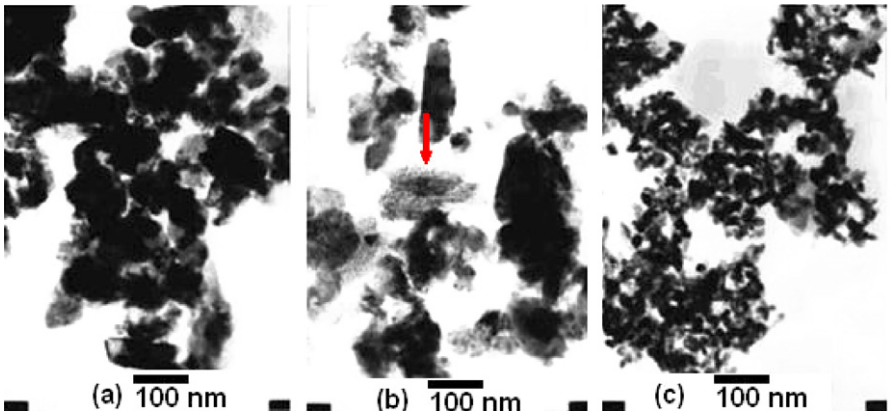

Fig. 3. TEM images of the original and the treated MgO samples under the flowing gaseous mixture of steam/CO_2/N_2 (CO_2/N_2 = 15/85 volume ratio) – (a) M0: original sample (b) M2: 700 °C, 12 h (c) M3: 700 °C, 24 h.

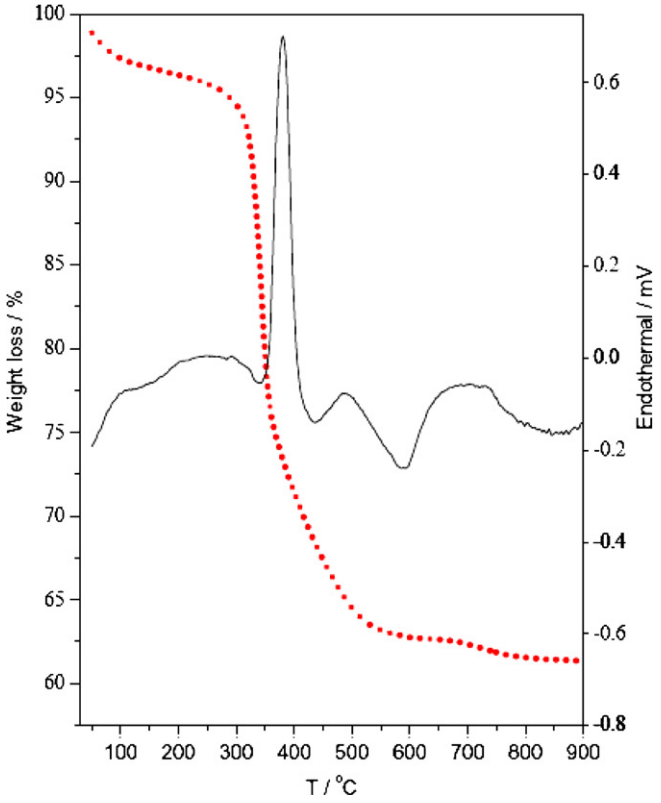

Fig. 4. TG-DTA curves of the carbonate precursor.

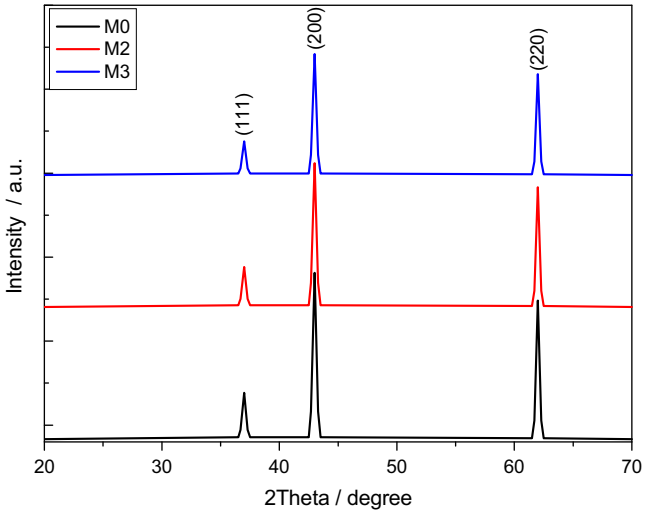

Fig. 5. XRD patterns of the MgO samples under the flowing gaseous mixture of steam/CO_2/N_2 (CO_2/N_2 = 15/85 volume ratio): (a) M0 (b) M2 and (c) M3.

endothermic peak in DTA curve. Secondly, a large weight loss (35 wt%) between 250 and 500 °C was caused by the combustion of the Span80 surfactant and the dehydroxylation, in which the former process is largely exothermic and but the latter is slightly endothermic; as a result, a large exothermic peak in DTA curve could be observed. Lastly, above 500 °C, there is a slight weight loss in TG curve due to the decomposition of carbonate, accompanied by an obvious endothermic peak in DTA curve. This suggests that carbonate decomposed completely into MgO at 750 °C. Therefore, the treatment with the gaseous mixture was carried out at 700 °C.

The crystal structures of the original and treated samples were further characterized by XRD. As shown in Fig. 5, all the samples crystallized perfectly with a cubic structure (JCPDS 4-0829), and no any other crystal phases (e.g. Mg $(OH)_2$ and $MgCO_3$) can be observed. The XRD results demonstrated that such treatment has no obvious influence on the MgO crystal structure. Supported by TEM micrographs, nevertheless, the treatments resulted in a decrease of the particle size and a significant increase in the surface area. The results calculated by Scherrer equation showed that the crystal sizes of M0, M2 and M3 are 25.5, 25.5 and 20.1 nm, respectively. Comparing M3 with M0, it seems that the crystals became smaller, although no obvious variation for M2. Besides, the contrast experiment showed that if only steam was used to treat the sample, the MgO sample sintered severely and its surface area has decreased to 27.1 $m^2\ g^{-1}$. It is well known that the presence of steam can accelerated the sintering of the particles. These results indicate that an underlying interaction mechanism may have been present in the process.

It is well known that the acid treatment of clays and natural silicates has long been studied with the intention of modifying the texture and acidity [12–21]. It has been reported that the surface of clay minerals can be modified through appropriate acid treatment, which leads to an increase in the surface area and/or in the number of acid centers. The surfaces of many metal oxides exhibit both Lewis base and/or Lewis acid character. These solid acid/base properties are particularly strong at corner/edge sites [22]. Residual surface hydroxyls and cation/anion vacancies can also add to the rich surface reactivities. Considering the base surface of MgO crystals and the acidic properties of CO_2 in the presence of steam [5], it could be tentatively assumed that the interaction processes may have taken place under the treatment conditions. In the presence of CO_2 and steam, the surface of the MgO particle was attacked by steam and CO_2. It seems that the instant "$MgCO_3$" intermediate may be metastable since the "$MgCO_3$" intermediate could not be present for a long duration at 700 °C (the temperature of carbonate decomposition), and it may decompose quickly into the MgO crystals. This process is described as the dynamic balance reaction below:

$$\begin{aligned} H_2O(g) + CO_2(g) + MgO &\leftrightarrow \text{“}MgCO_3\text{”} + H_2O(g) \\ &\leftrightarrow MgO + CO_2(g) \\ &\quad + H_2O(g) \end{aligned} \tag{1}$$

Indeed, on base of the TG-DTA results above, it is possible that there is a dynamic balance between the surface reaction and the decomposition in the presence of CO_2 and steam at 700 °C. Under the conditions, it could be

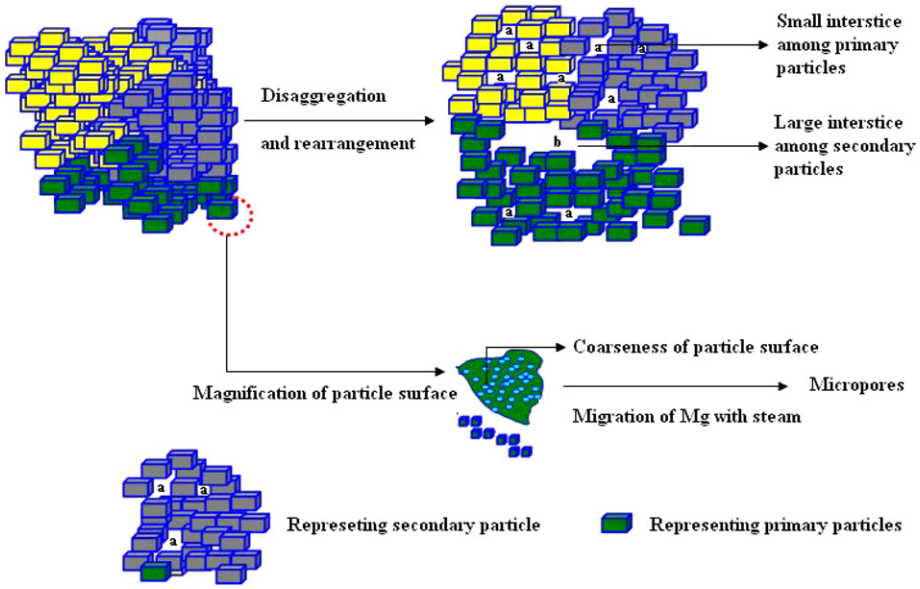

Fig. 6. The schematic rearrangement process of the MgO particles.

assumed that the former process may be much slow and the latter may be much fast, and the small MgO grains were formed.

MgO belong to a perfect cubic crystal. During the process, we assumed that attached by CO_2 and steam, several factors should be involved in this process: First, the surfaces of MgO grains would become coarse, which could contribute to the increase of its BET surface area. Second, the process is complicate. It is understandable that some large secondary particles would redisperse or disaggregate. As a result, the primary particles would rearrange to form the new secondary particles. The 3.9 nm (and 2.8 nm) pores may result from the interstices within secondary particles, which contributes to the increase of the BET area and the variations of the pore size of the sample. Third, the Mg on the surface of the sample would migrate with the steam, and formed small grains or grew into large ones. Moreover, the migration of Mg from the grain surface, some micropores would generate, resulting in the increase of micropores. All these may also favor for the increase of the BET area and the variations of pore size. The sketched diagram of the restructured particles is shown in Fig. 6.

3.3. Catalytic combustion of methane

The catalytic properties of the MgO sample may be affected by the textural properties and the particle sizes. The combustion of methane was conducted over the MgO samples. The light-off curves for methane combustion are shown in Fig. 7. After treatment, the ignition temperature (T_{10}) and the complete combustion temperature (T_{90}) over the M3 sample were 690 and 790 °C, but those over the original one (M0) were 710 and 830 °C, respectively. Both MgO samples showed the higher activities than

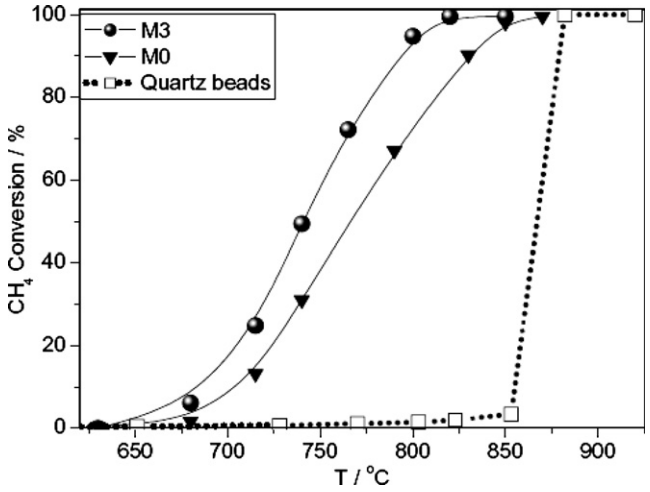

Fig. 7. Light-off curves of methane combustion over the MgO samples.

the quartz bead ($T_{10} = 850$ °C, $T_{90} = 880$ °C), which could be attributed to their higher surface areas (37.9 and 80.1 $m^2\ g^{-1}$) than that (3.1 $m^2\ g^{-1}$) of the quartz bead. It is well known that at low conversions of methane, methane combustion is mainly controlled by surface catalytic reaction [23]. The adsorption of the reacting gases may have a significant influence on the catalyst activity. After treatment, the MgO sample with large surface area may favor for the adsorption of the reactants, which promoted the surface reaction.

Importantly, the T_{90} difference (40 °C) of both MgO samples was much lager than their T_{10} difference (20 °C). It is well known that at high conversions of methane, the oxidation of methane usually includes surface reaction and free radical reaction [23]. The free radical reactions are more dependent on mass transfer than on the surface reaction. Before the gases reacted on the solid surface,

the gas diffusion from bulk gases to the solid surface occurred. Because the surface reaction is relative fast, the influence of mass transfer from gas bulk to the catalyst surface on the reaction should not be ignored. The surface reaction and mass transfer may be affected by various factors, e.g., intrinsic activity, particle sizes, porosity and concentration of catalyst [23]. Considering the non-variable valence of Mg ions, the intrinsic activity of MgO is very low, the influence of textural properties of the MgO sample on the mass transfer process may be more significant than on the surface reaction. The large surface area of the catalyst is beneficial to mass transfer, since the large surface area may favor for the adsorption of more gases on the solid surface. As a result, the T_{90} difference (40 °C) of the both MgO samples was much lager than their T_{10} difference (20 °C).

4. Conclusions

By treatment under the flowing gaseous mixture of steam and CO_2, the surface area of the MgO sample can be increased significantly, the maximum of pore size distribution varied and the pore volume increased. The variations of textural properties were mainly ascribed to the disaggregation and rearrangement of the MgO particles. As a result, the MgO sample after treatment showed a higher activity than the original one. This treatment method may be also used to regenerate or investigate the other catalysts/supports.

Acknowledgments

We thank the financial support provided by Chinese National Science Foundation (Nos. 20433010 and 20571047), Chinese Postdoctoral Science Foundation (Grant 20060390057), and the 973 Great Foundation Project of China (G1999022401).

References

[1] L.D. Pfefferle, W.C. Pfefferle, Catal. Rev. Sci. Eng. 29 (1987) 219.
[2] H. Tsuji, F. Yagi, H. Hattori, H. Kita, J. Catal. 148 (1994) 759.
[3] B. Soylu, N. Adamopoulos, D.M. Glowacka, J.E. Evetts, Appl. Phys. Lett. 60 (1992) 22.
[4] P. Yang, C.M. Lieber, Science 273 (1996) 1836.
[5] G.A.H. Mekhemer, S.A. Halawy, M.A. Mohamed, M.I. Zaki, J. Phys. Chem. B 108 (2004) 13379.
[6] K. Hirota, N. Okabayashi, K. Toyoda, O. Yamaguchi, Mater. Res. Bull. 27 (1992) 319.
[7] J. Green, J. Mater. Sci. 18 (1983) 637.
[8] Y. Diao, W.P. Walawender, C.M. Sorensen, K.J. Klabunde, T. Ricker, Chem. Mater. 14 (2002) 362.
[9] V. Štengl, S. Bakardjieva, M. Maříková, P. Bezdička, J. Šubrt, Mater. Lett. 57 (2003) 3998.
[10] R. Richards, W. Li, S. Decker, C. Davidson, O. Koper, V. Zaikovski, A. Volodin, T. Rieker, K.J. Klabunde, J. Am. Chem. Soc. 122 (2000) 4921.
[11] K.S.W. Sing, D.H. Everett, R.A.W. Haul, L. Moscow, R.A. Pinerotti, J. Rouquerol, T. Siemieniewska, Pure Appl. Chem. 57 (1985) 603.
[12] J.de D. López González, A. Ramírez, F. Rodríguez Reinoso, C. Valenzuela Calahorro, L.Z. Herrera, Clay Miner. 16 (1981) 103.
[13] S. Mendioroz, J.A. Pajares, I. Benito, C. Pesquera, F. Gozález, C. Blanco, Langmuir 3 (1987) 676.
[14] C. Pesqura, F. González, I. Benito, C. Blanco, S. Mendioroz, J.A. Pajares, J. Mater. Chem. 2 (1992) 907.
[15] M.A. Vicente Rodríguez, J. de D. López González, M.A. Banares Munoz, Clay Miner. 29 (1994) 361.
[16] A.N. Shigapov, G.W. Graham, R.W. McCabe, M.P. Peck, H.K. Plummer, Appl. Catal. A 182 (1999) 137.
[17] T.H. Elmer, Ceram. Eng. Sci. Proc. 7 (1986) 40.
[18] M.A.I. Duarte, J.C.D. Macedo, D.B. Alves, in: Proceedings of the 10th International Clay Conference 1993/Pub. P.112, 1995.
[19] B. Suna, J. Chem. Technol. Biotechnol. 66 (1) (1996) 72.
[20] J. Aznar, E. Gutierrez, P. Diaz, A. Alvarez, G. Poncelet, Micropor. Mater. 6 (2) (1996) 105.
[21] M.A. Vicente Rodriguez, J. de Lopez Gonzales, M.M. Banares Munoz, Micropor. Mater. 4 (1995) 251.
[22] E. Knozinger, K.H. Jakob, S. Singh, P. Hoffman, Surf. Sci. 290 (1993) 288.
[23] E.M. Johansson, K.M.J. Danielsson, E. Pocoroba, E.D. Haralson, S.G. Järäs, Appl. Catal. A: Gen. 182 (1999) 199.